

Fast-Tracking Space Charge tool for Nonlinear Dynamics study in Realistic Collider Lattices

Helena Alamprese, Yue Hao

Beam Dynamics Group MSU





This material is based upon work supported by the U.S. Department of Energy, Office of Science, Office of Nuclear Physics and used resources of the Facility for Rare Isotope Beams (FRIB) Operations, which is a DOE Office of Science User Facility under Award Number DE-SC0023633.

Contents

- Motivation and background – Space Charge effects in high intensity accelerators.
- 2.5D Space Charge models and GPU implementation.
- Potential Fast-tracking tool using a Symplectic Neural Network surrogate model.
- Conclusions.

Background and Motivation

- Since the early 1980s, the Intensity and brightness frontier pushing for higher luminosity, has revealed limiting factors like beam halo and emittance growth related to space charge force.
- The computational challenge: Poisson solvers and PIC techniques are computationally expensive for multiturn studies.
- The aim of this work is to develop an efficient tracking solution for the phase-space evolution of beams subject to space charge in real nonlinear lattices.
- Fast-tracking solutions will be beneficial to high-intensity machines simulations (e.g., SuperKEKB, EIC, Muon Colliders, Spallation neutron sources).

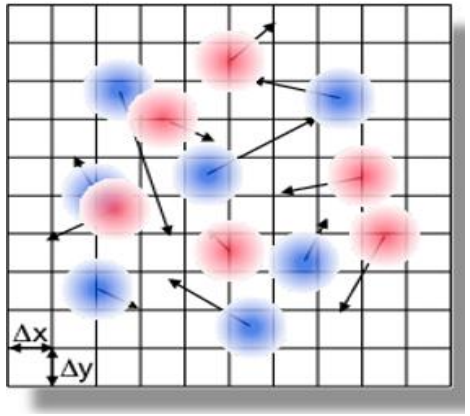


Fig.1 Example of a PIC grid.

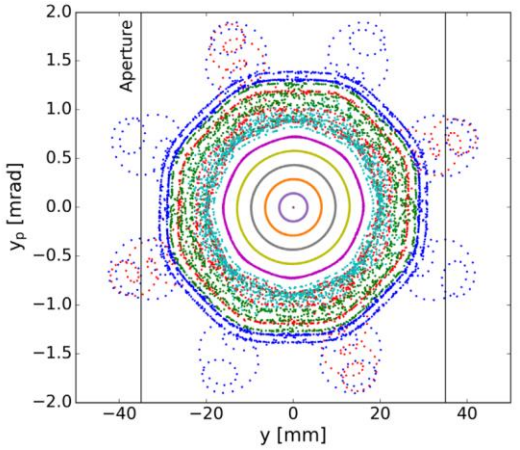


Fig.2 Identification of resonances on vertical phase space [1].

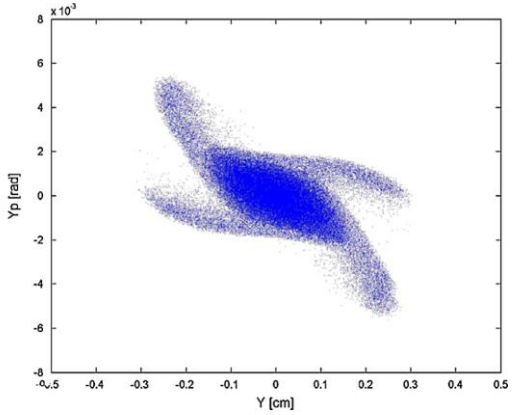


Fig.3 Beam distribution when particles cross the $4\sigma = 360°$ resonance [2].

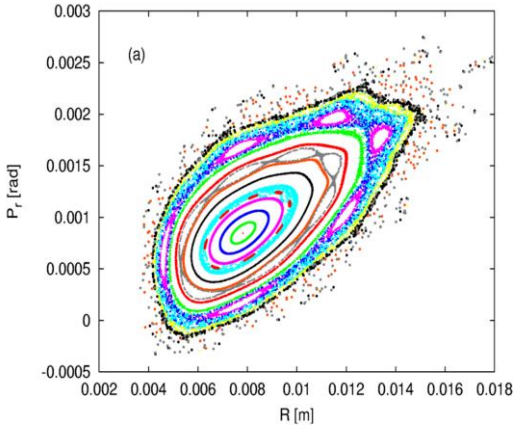


Fig.4 Vertical envelope in The Proton Storage Ring (PSR - Los Alamos National Laboratory) lattice [3].

[1] Bartosik et al. "Space charge induced losses in the CERN injector complex." Journal of Instrumentation 15, no. 07 (2020): P07021-P07021.
[2] Jeon, Dong-O. et. al. "Fourth order resonance of a high intensity linear accelerator." Physical Review Special Topics—Accelerators and Beams 12, no. 5 (2009): 054204.
[3] Cousineau, et al. "Space charge induced resonance excitation in high intensity rings." Physical Review Special Topics—Accelerators and Beams 6, no. 3 (2003): 034205

2.5D Space Charge model for bunched beam

- The transverse density distribution can be approximated as a bi-gaussian distribution. The 2.5D space charge model is valid if

$$\frac{\partial^2 \varphi}{\partial x,y^2} \gg \frac{1}{\gamma^2} \cdot \frac{\partial^2 \varphi}{\partial z^2}$$

- Consequently, the transverse momenta acquire the z-dependence through λ_z linear charge distribution

$$\rightarrow \; Q\,\lambda_z = Q\,\frac{e^{-z^2/2\sigma_z^2}}{\sigma_z\sqrt{2\pi}}$$

- The map satisfies the symplectic condition: $M^T J M = J$ with

$$J = \begin{pmatrix} 0 & I_n \\ -I_n & 0 \end{pmatrix}$$

Space charge kick momentum

$$\begin{pmatrix} dp_x = KE_x(r)\,\lambda(z)\,ds \\ dp_y = KE_y(r)\,\lambda(z)\,ds \\ dp_z = -K(\varphi(x,y) + \varphi_{00})\,\frac{d\lambda(z)}{dz}\,ds \end{pmatrix}$$

with $\varphi_{00}(x=0,y=0) = -\frac{1}{4\pi\varepsilon_0}\left[\log 2 - \gamma_{em} + 2\log\left(\frac{\sigma_x+\sigma_y}{2}\right)\right.$ [6]

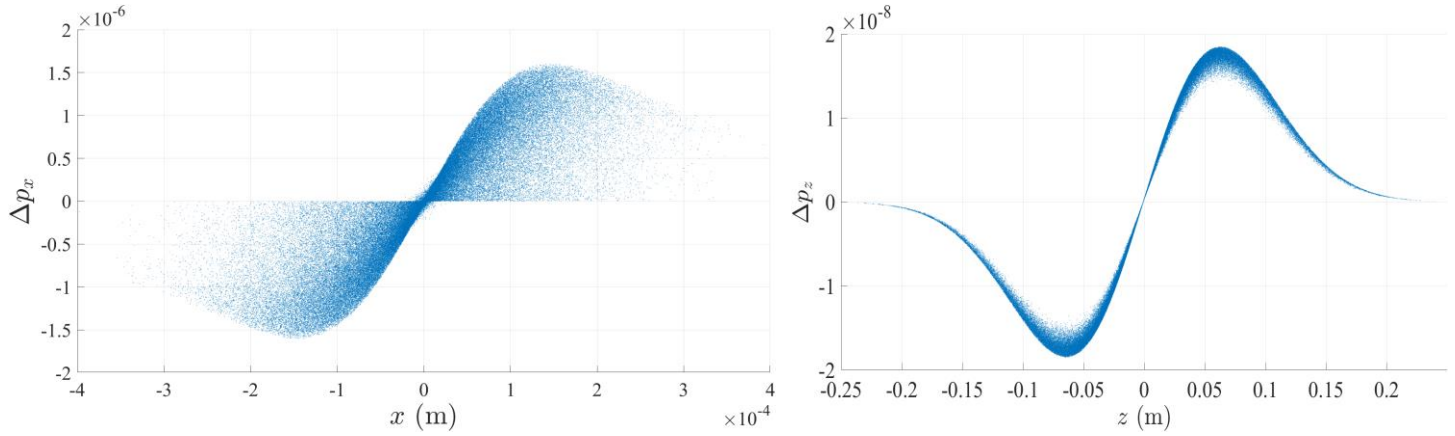


Figure 5. Horizontal (left) and longitudinal (right) Space Charge kick momentum.

[6]] Qiang, Ji. 2025. "Two-and-a-Half Dimensional Symplectic Space-Charge Solver." *Physical Review Accelerators and Beams* 28 (11): 114602

GPU Implementation

- Element-wise simulations with parallel execution: custom GPU kernels map individual threads to distinct macroparticles, ensuring highly efficient $O(N)$ phase-space updates.

- The Faddeeva function (Error function) is the main limit for space charge and beam-beam evaluations. It accounts for around 80% of the simulation time. Speeding up simulation time means optimizing the Faddeeva function (work from Brookhaven National Lab) [9].

- The simulation time decreased by a factor 2.5 thanks to the optimization of the Faddeeva function.

- The **Wiedemann algorithm** is

$$\left(\frac{1}{c(z)} \cdot \sum_{n=0}^{N-1} a_n b^n(z) + d\right) \cdot \frac{1}{c(z)}$$

- Use **Horner's rule** for the polynomial part

$$\rightarrow a_0 + b(z)\left[a_1 + b(z)\left(a_2 + \cdots + b(z)(a_{N-2} + b(z)\, a_{N-1})\right)\right]$$

- Apply metaprogramming ("a code which writes a code")
- **Precompute the coefficients** $\{a_n\}_{n=0}^{N-1}$. In Julia, it is possible to pre-compute them at compile time for arbitrary N.
- **Unroll the expression**: instead of looping over polynomial terms, generate explicit nested expressions.
- **Use Fused Multiply-Add (FMA)** instruction. Modern CPUs/GPUs support FMA, which computes $x \cdot y + z$ in a single step. [9]

[9] https://github.com/ykkan/WSTrack.jl

Data treatment and strategy

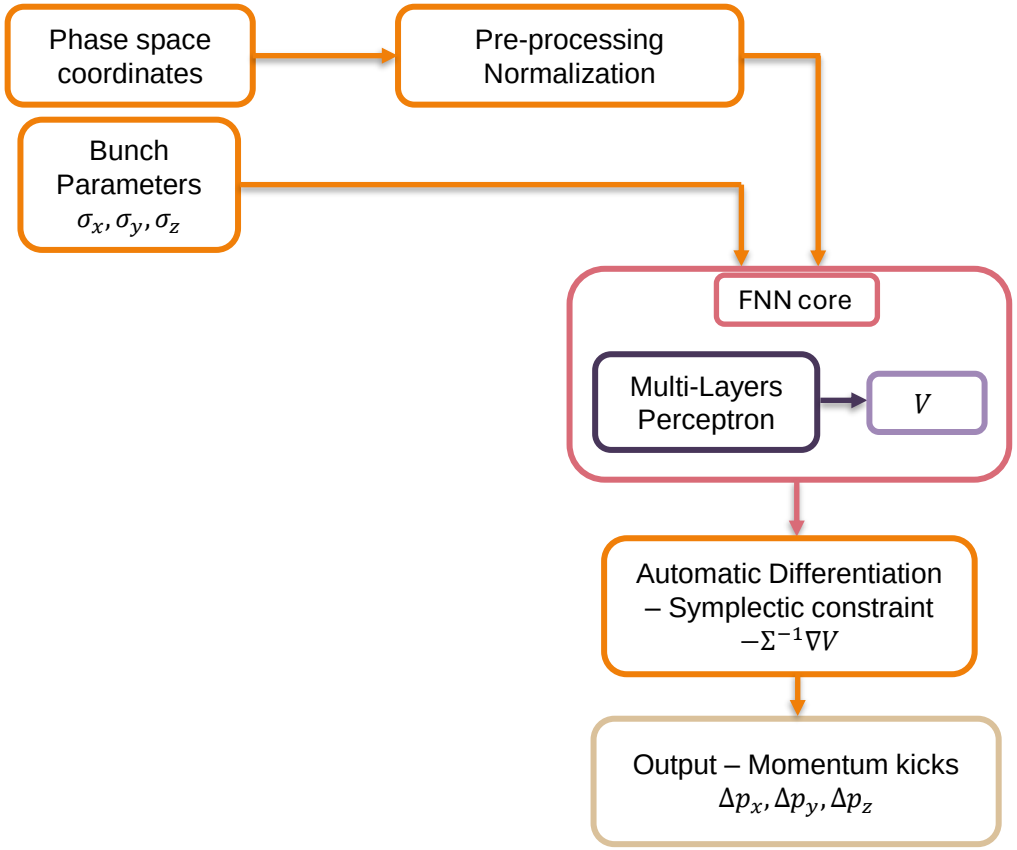
- The GPU code has been used to generate the beam phase space data for training, validation and testing datasets.

1. Hundreds of gaussian bunched beam phase spaces (with 100k macro particles) are generated with random $\sigma_{x,y,z}$ while ensuring the condition for the 2.5D model: $\frac{\delta^2\varphi}{\delta x,y^2} \gg \frac{1}{\gamma^2}\frac{\delta^2\varphi}{\delta z^2}$.
2. The particles belong to a specific beam distribution, and the particle identity is conserved for the training, testing and validation datasets.
3. Consider the relationship between the particles in each beam and the kick they experience. Normalization with respect to $\sigma_x, \sigma_y, \sigma_z$ is required $\left(F_{sc} \propto \frac{1}{\sigma_x \sigma_y}\right)$.
4. Therefore, the phase space coordinates can be defined as

$$\boldsymbol{q} = [x, y, z]^T \rightarrow \hat{\boldsymbol{q}} = \boldsymbol{\Sigma}^{-1}(\boldsymbol{q} - \boldsymbol{\mu_q})$$
$$\boldsymbol{\lambda} = [\sigma_x, \sigma_y, \sigma_z]$$
$$\boldsymbol{h}^{(0)} = [\hat{\boldsymbol{q}}^T \ \boldsymbol{\lambda}^T]^T$$

Symplectic Normalization

$$\begin{cases} Q = \frac{q}{\sigma} \\ P = p * \sigma \end{cases} \rightarrow Q \cdot P = q \cdot p$$



Symplectic FNN structure

- The FNN is constructed as a Multi-Layer Perceptron (MLP) with L –hidden layers. It maps the high-dimensional input vector to a single, unitless scalar potential V

$$\mathrm{F}(x.y,z) \rightarrow V(q) \rightarrow F'(\Delta p_x, \Delta p_y, \Delta p_z)$$

- With $l \in \{1,2,\dots,N_L\}$ hidden layers, the forward propagation is defined by a linear transformation followed by a non-linear activation function φ ($\tanh(\cdot)$ for this test).

$$h^{(l)} = \varphi\left(W^{(l)}h^{(l-1)} + b^{(l)}\right)$$

with
- $W^{(l)}$: learnable weight matrices
- $b^{(l)}$: bias vectors
- $h^{(l-1)}$: previous layer outputs

- The losses are calculated through the MSE loss function.

$$\mathcal{L} = \frac{1}{N}\sum \left\| \Delta p_{true} - \left(\underbrace{-\Sigma^{-1}\nabla_{\hat{q}}V}_{\Delta p_{pred}}\right)\right\|^2$$

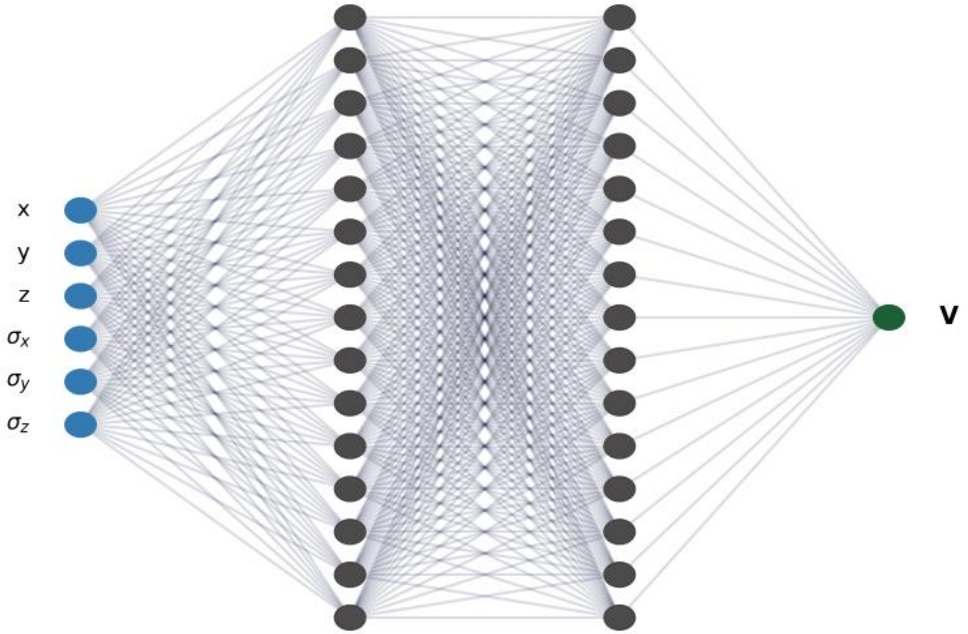


Fig.6 Multi-Perceptron layers diagram.

$$V\left(\hat{\boldsymbol{q}}, \boldsymbol{\lambda}; \left(\boldsymbol{W}^{(l)}, b^{(l)}\right)\right) = \boldsymbol{W}^{(L+1)}\boldsymbol{h}^{(L)} + b^{(L+1)} \rightarrow \Delta \boldsymbol{p} = -\nabla_q \boldsymbol{V}$$

$$\nabla_{\boldsymbol{q}}\boldsymbol{V} = \left(\frac{\partial \hat{\boldsymbol{q}}}{\partial \boldsymbol{q}}\right)^T \nabla_{\hat{\boldsymbol{q}}}\boldsymbol{V} \rightarrow$$

$$\Delta \mathbf{p} = -\boldsymbol{\Sigma}^{-1}\nabla_{\hat{\boldsymbol{q}}}\boldsymbol{V}\left(\hat{\boldsymbol{q}}, \boldsymbol{\lambda}; \boldsymbol{W}^{(l)}\boldsymbol{b}^{(l)}\right)$$

Symplectic FNN as a Surrogate model

- The surrogate model successfully captures the sharp, non-linear physical gradients near the beam core.
- Tight clustering along the red dashed line indicates highly accurate individual particle predictions (Fig.7).
- 2D cross-sections of the beam phase-space demonstrate accurate kick predictions across the bunch volume.
- RMS error (bottom row in Fig.8) confirms that the model maintains good precision directly through the high-density beam core.
- Relative Error (top row in Fig.8): errors are low except for the center high-error lines which are mathematical artifacts (divide-by-zero effect at center).

$$\text{Relative Error} = \frac{|dp_{pred} - dp_{true}|}{dp_{true}}$$

$$RMSE = \sqrt{\frac{1}{N}\sum_{i=1}^{N}\left(dp_{pred,i} - dp_{true,i}\right)^2}$$

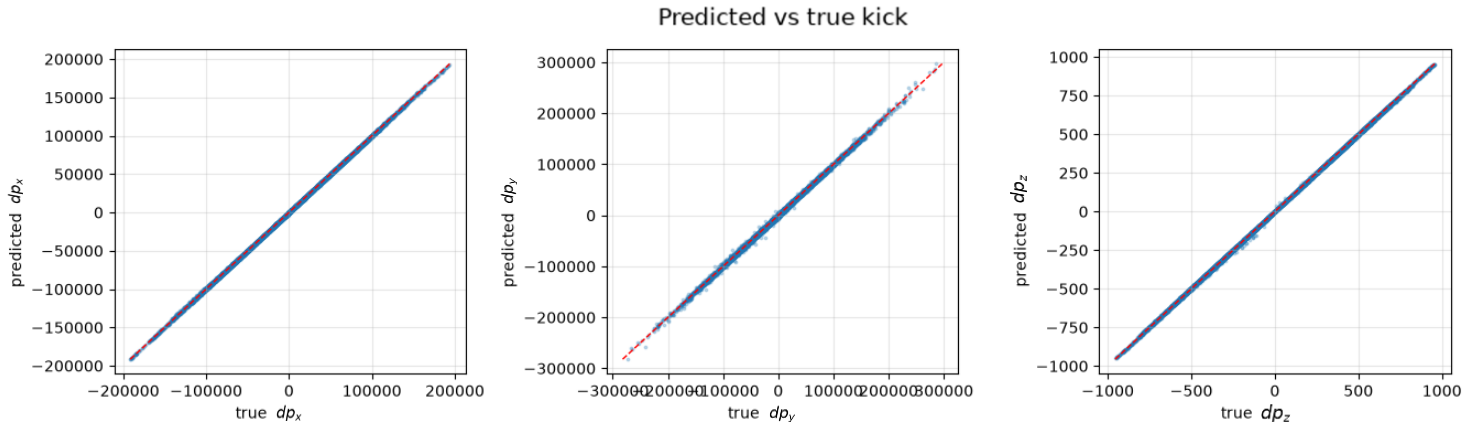


Fig.7. Correlation between predicted and true momentum kicks across all three dimensions.

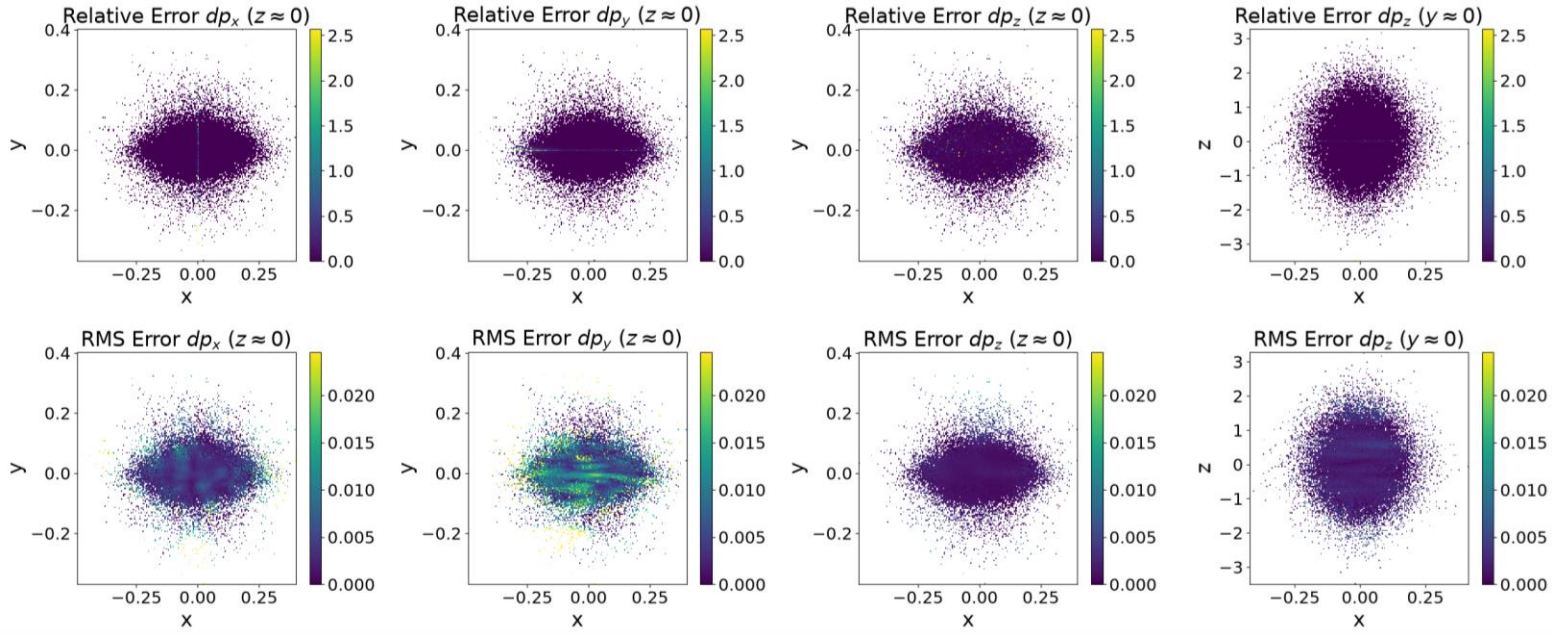


Fig.8 2D Spatial Error distribution. The heatmap represents the Relative (top) and RMS errors (bottom).

FODO cell beam dynamics simulations

- The surrogate model has been implemented in beam tracking code for testing it in a simple FODO cell.
- The simulations demonstrate good agreement between analytical and neural network surrogate models, yielding consistent tune diagram results across varying space charge strength.
- The plots show results with different space charge strength:

$$\xi = \frac{N r_p}{4\pi \varepsilon_{x,y} \beta^2 \gamma^3}.$$

(a – b): $\Delta Q_{x,y} \propto 0.01 - 0.03$

(c – d): $\Delta Q_{x,y} \propto 0.001 - 0.003$

$$\Delta Q_{x,y} \propto -\frac{n}{\beta^2 \gamma^3 \sigma_z} \oint \frac{\beta_z}{\sigma_x(\sigma_x + \sigma_y)} ds$$

$$\rightarrow \Delta Q_x \propto -\frac{r_0 N C}{(2\pi)^{\frac{3}{2}} \beta^2 \gamma^3 \sigma_z \varepsilon_x} \left(\frac{1}{1 + \sigma_y/\sigma_x} \right)$$

- using average beam sizes and average beta functions

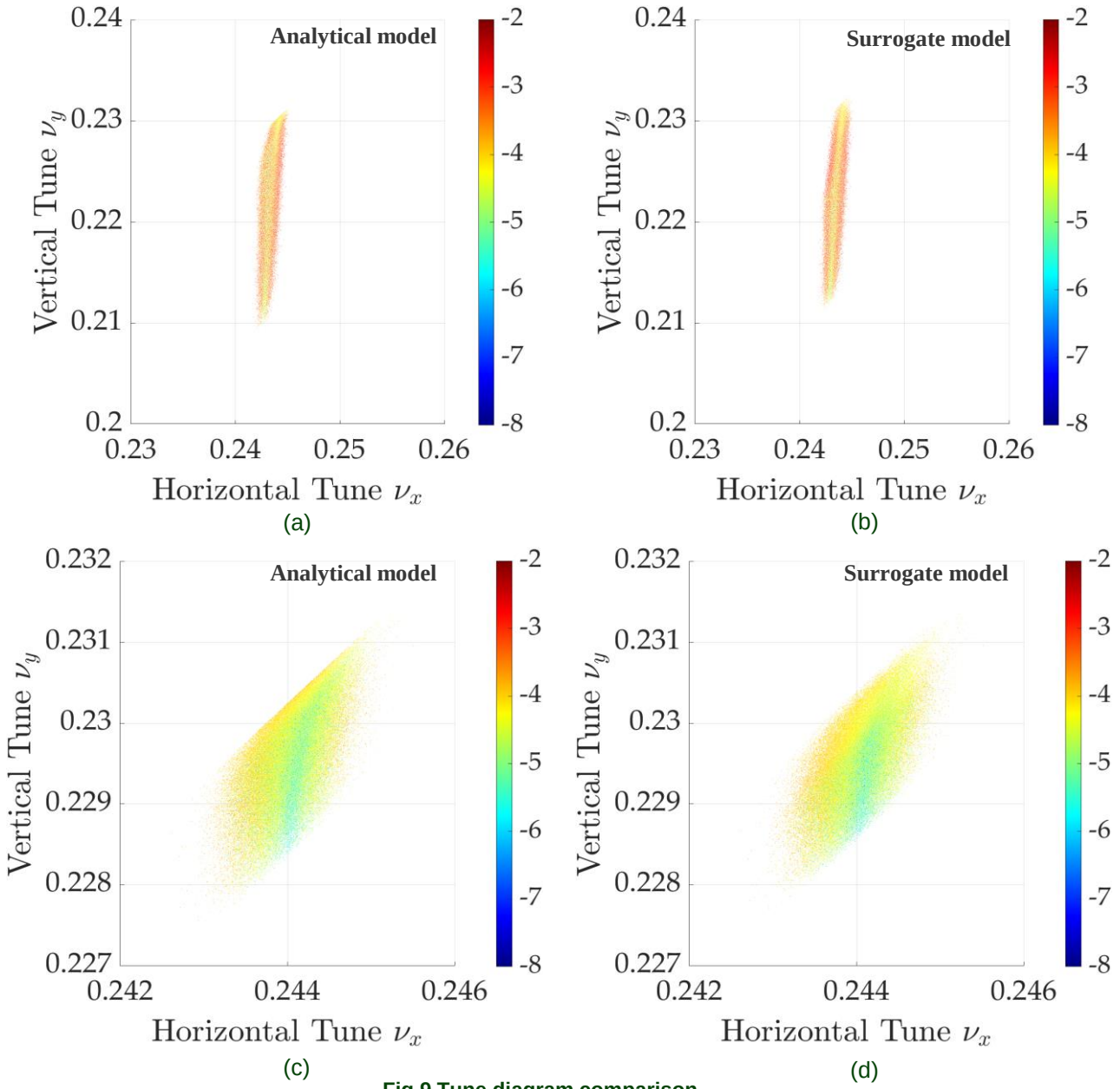


Fig.9 Tune diagram comparison.

FODO cell beam dynamics simulations

- Long-term tracking bunched beam study in a FODO cell demonstrates consistent beam size dynamics across the two models.
- Some discrepancies are evident for the vertical y-emittance and longitudinal emittance amplitude.
- Model trained on flat ratio $r = \frac{\sigma_y}{\sigma_x} \in [0.01 - 0.1]$ dataset. Results on a test beam with $r_{avg} = 0.1$
- $\Delta Q_{x,y} \propto 0.01 - 0.03$

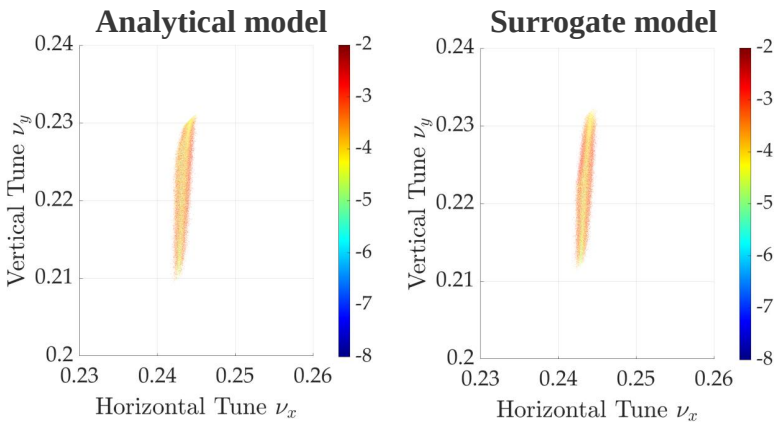


Fig.10Tune diagram comparison.

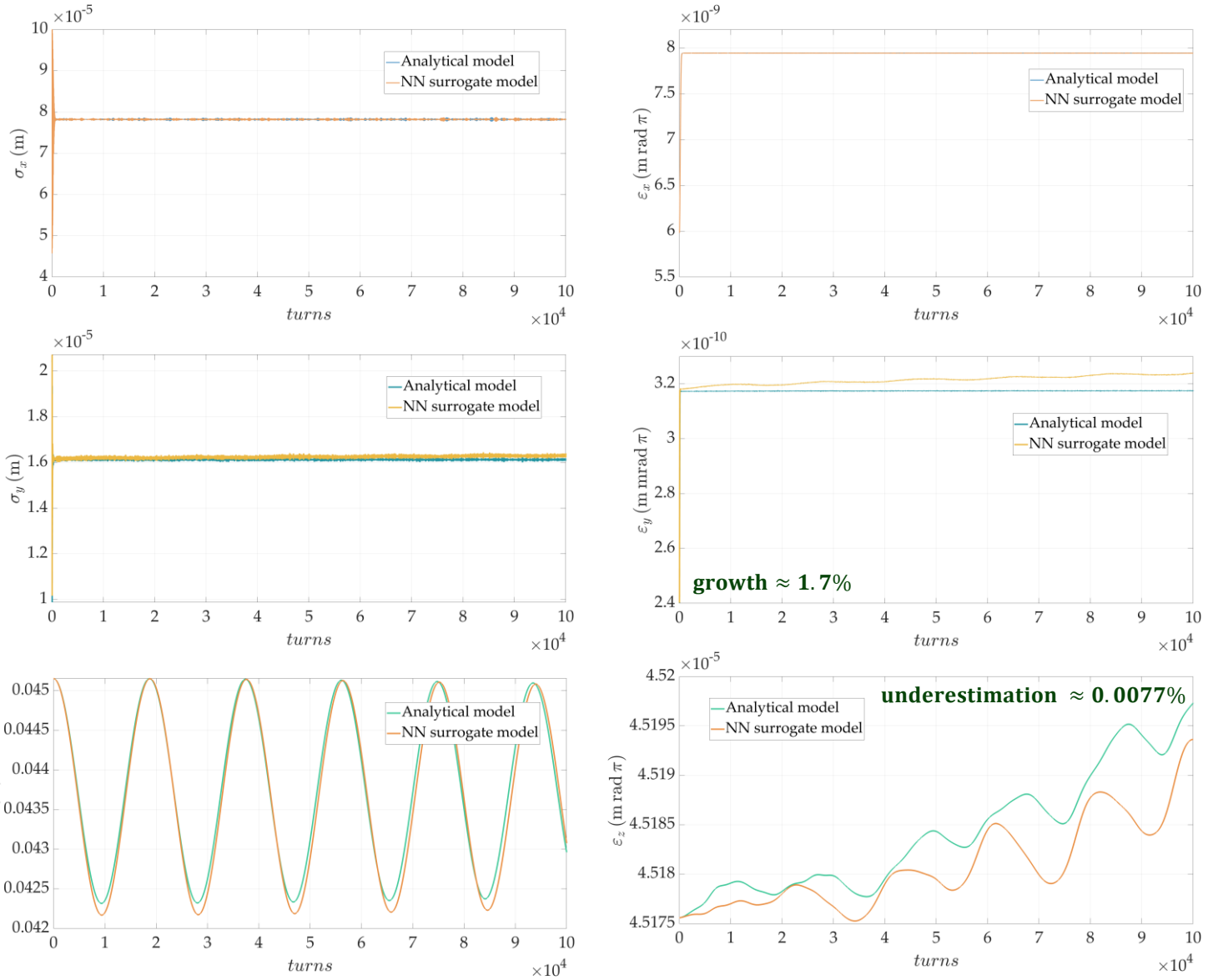


Fig.11 Envelope study, beam size and emittance evolution over 100,000 turns.

FODO cell beam dynamics simulations

- Space charge strength is approximately double that of the previous case – test for evaluating the limits of the surrogate model.

- Model trained on flat ratio $r = \frac{\sigma_y}{\sigma_x} \in [0.01 - 0.1]$ dataset. Results on a test beam with $r_{avg} = 0.1$

- $\Delta Q_{x,y} \propto 2 \cdot (0.01 - 0.03)$

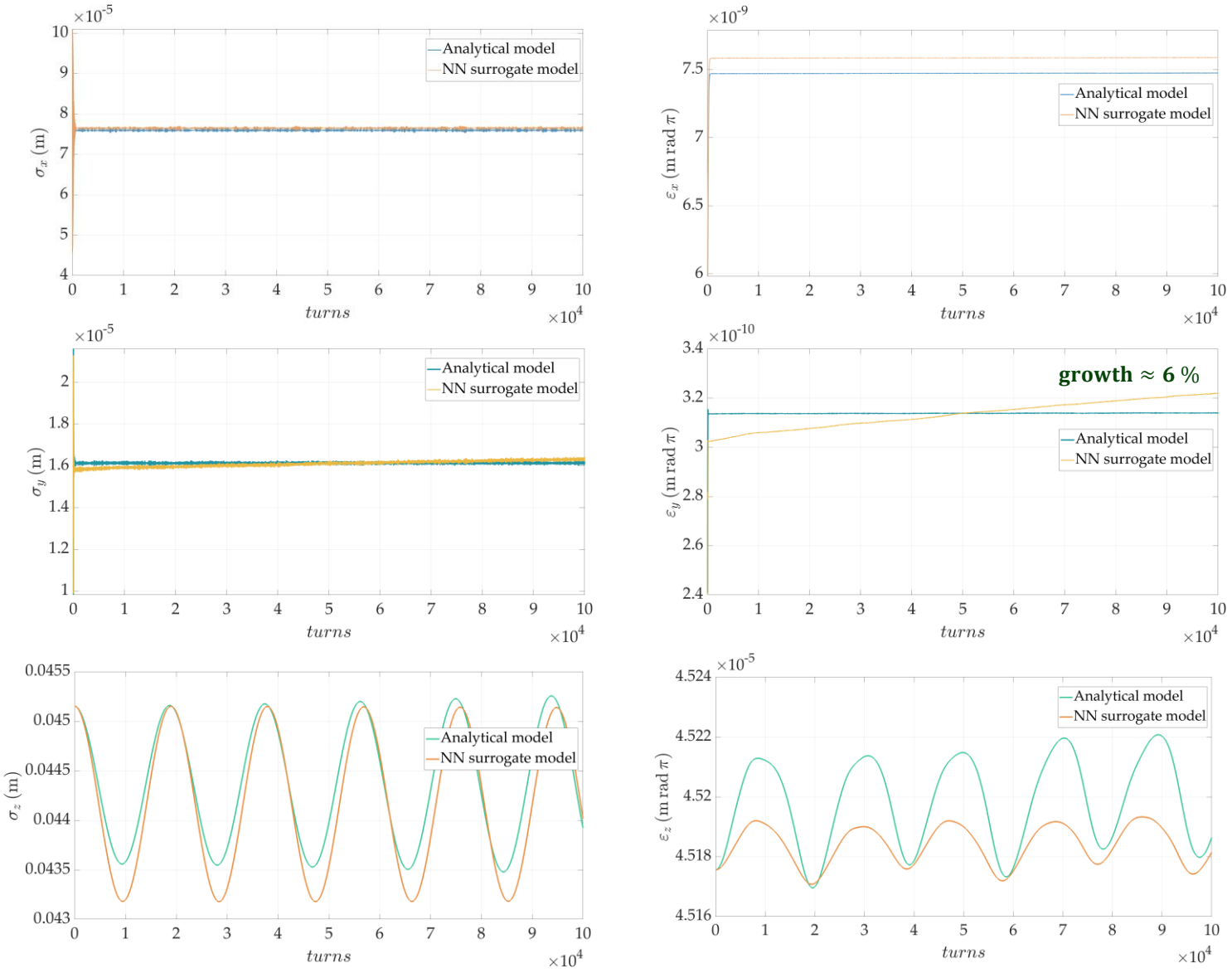


Fig.12 Envelope study, beam size and emittance evolution over 100,000 turns with doubled space charge strength.

FODO cell beam dynamics simulations

- Space charge stregth is approximately doubled than the previous case – test for evaluating the limits of the surrogate model.

- Model trained on flat ratio $r = \frac{\sigma_y}{\sigma_x} \in [0.1 - 0.9]$ dataset. Results on a test beam with $r_{avg} = 0.1$

- $\Delta Q_{x,y} \propto 2 \cdot (0.01 - 0.03)$

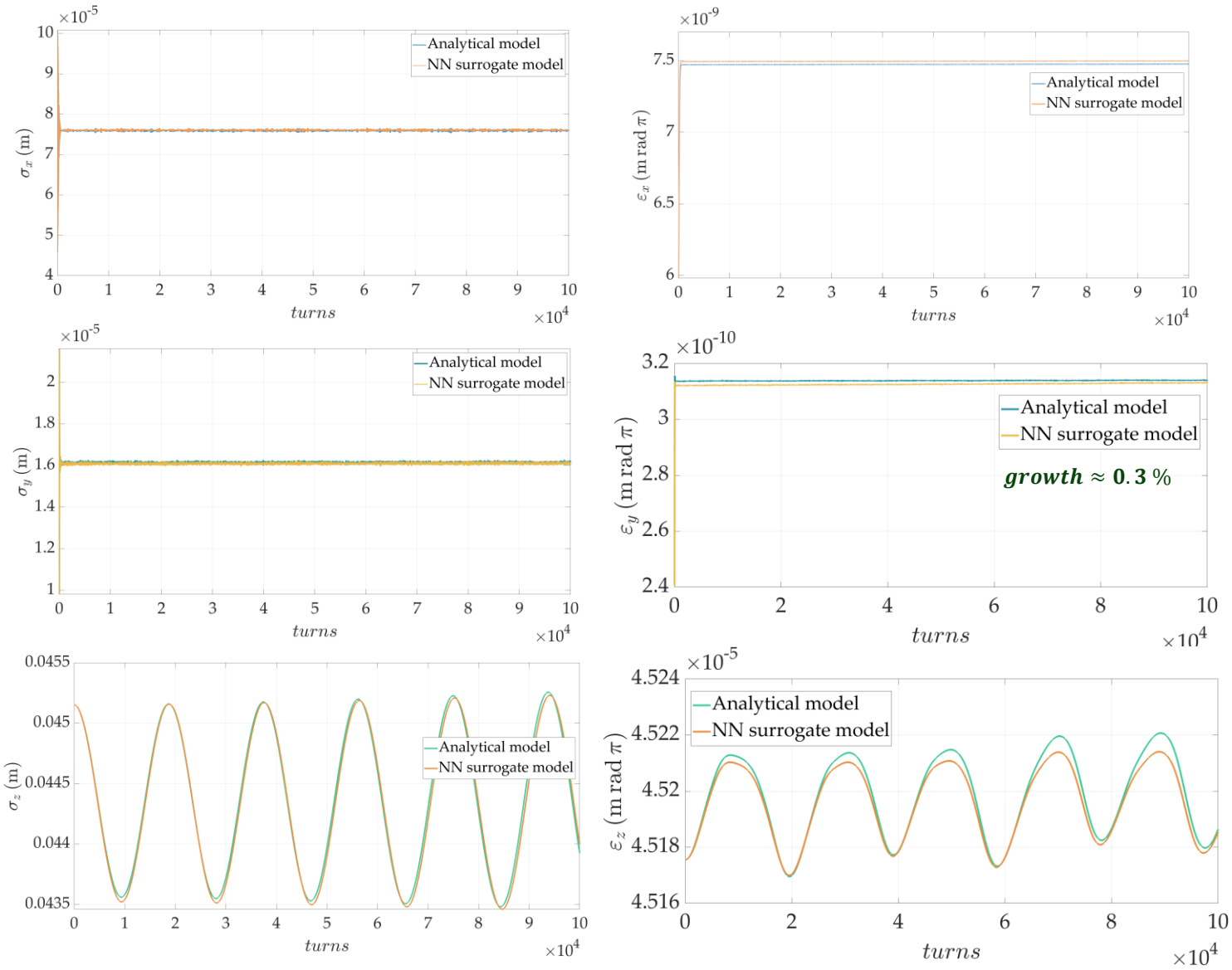


Fig.13 Envelope study, beam size and emittance evolution over 100,000 turns with doubled space charge force.

FODO cell beam dynamics simulations

- Space charge stregth is approximately one order higher than the default case – test for evaluating the limits of the surrogate model.
- Model trained on flat ratio $r = \frac{\sigma_y}{\sigma_x} \in [0.1 - 0.9]$ dataset. Results on a test beam with $r_{avg} = 0.1$
- $\Delta Q_{x,y} \propto 10 \cdot (0.1 - 0.3)$

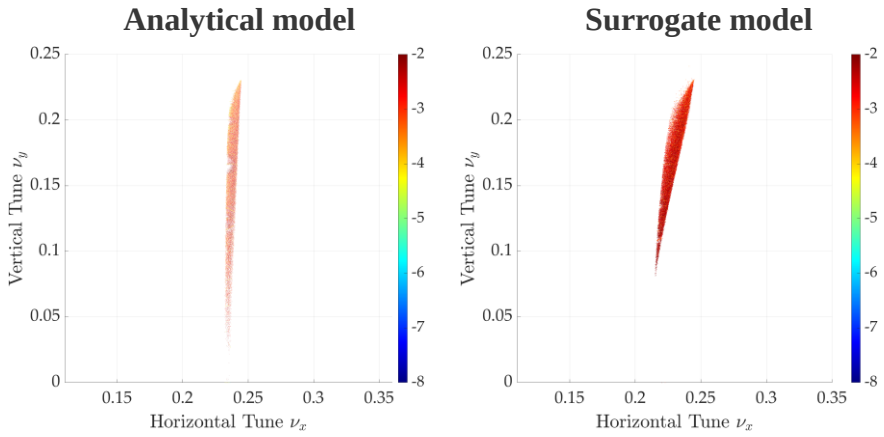


Fig.14 Tune diagram comparison.

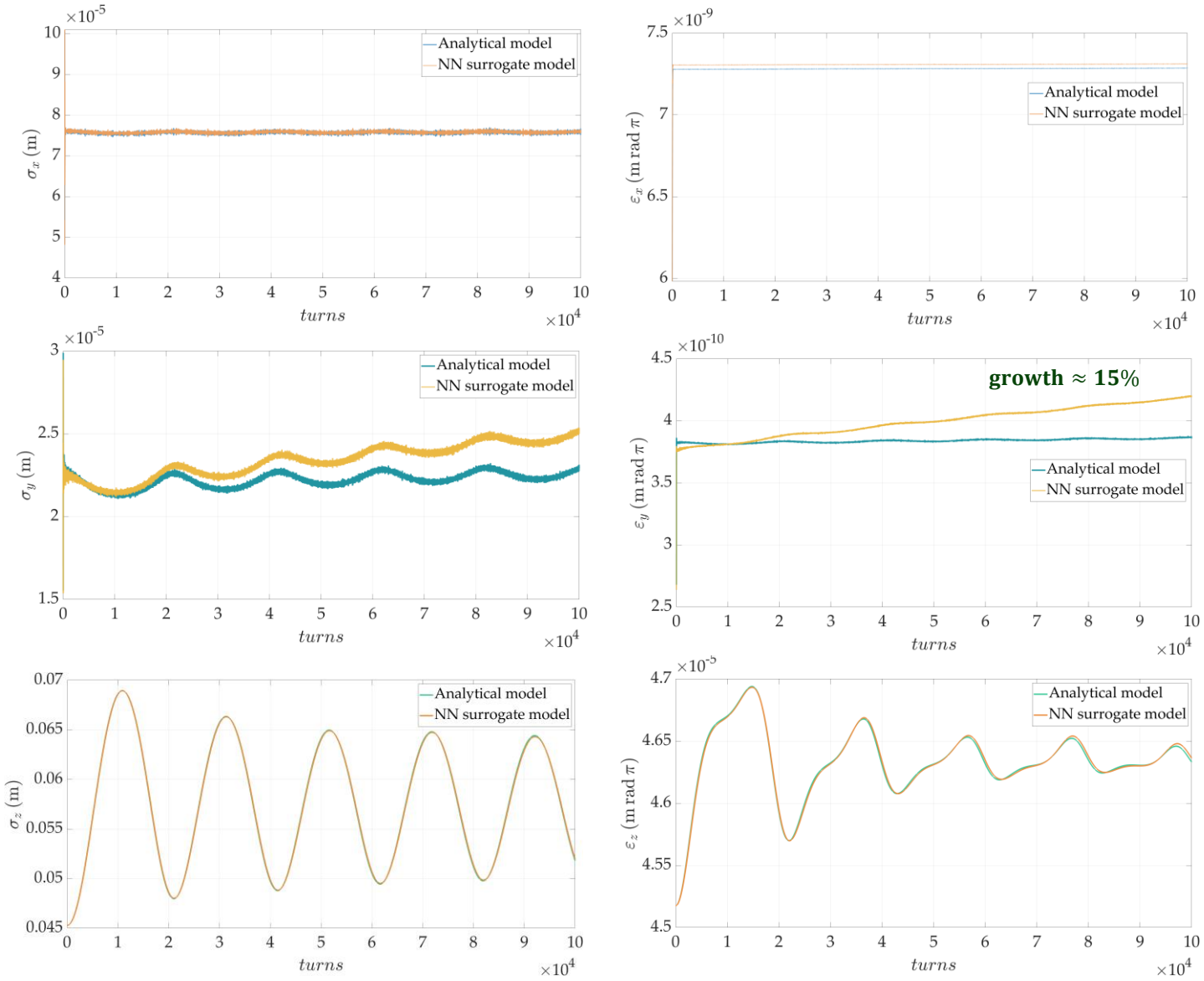


Fig.15 Envelope study, beam size and emittance evolution over 100,000 turns increasing 10x space charge force.

FODO cell beam dynamics simulations

- Model trained on flat ratio $r = \frac{\sigma_y}{\sigma_x} \in [0.1 - 0.9]$ dataset. Results on a test beam with $r_{avg} = 0.5$

- $\Delta Q_{x,y} \propto (0.004 - 0.004)$

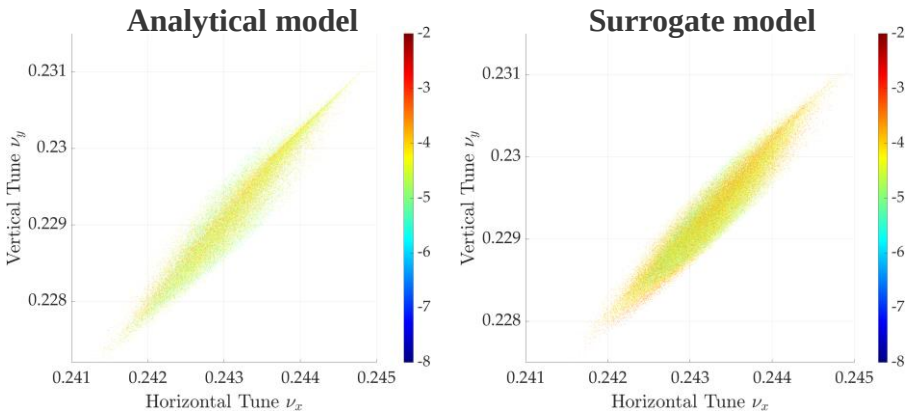


Fig.16 Tune diagram comparison.

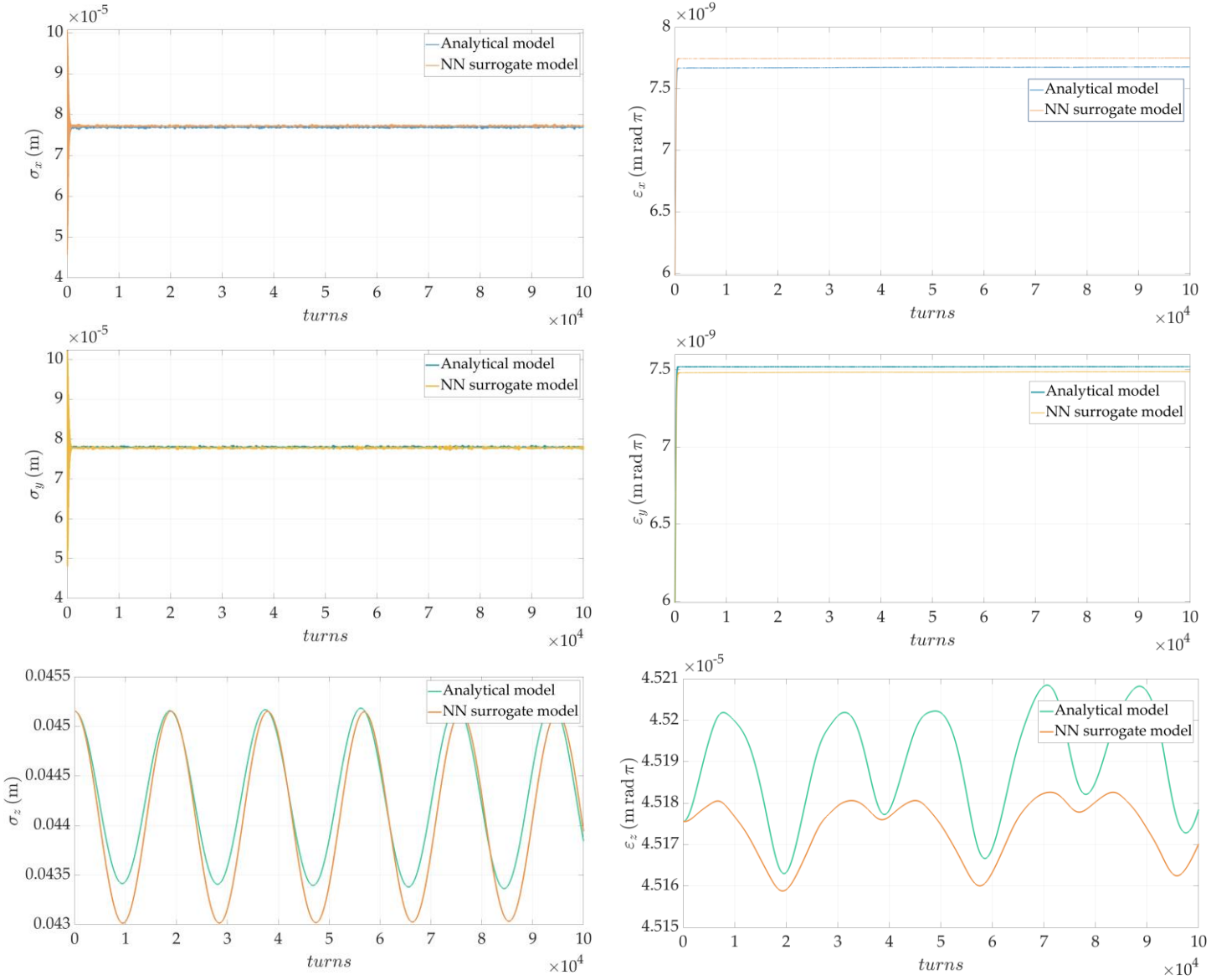


Fig.17 Envelope study, beam size and emittance evolution over 100,000 turns.

FODO cell beam dynamics simulations

- Model trained on flat ratio $r = \frac{\sigma_y}{\sigma_x} \in [0.1 - 0.9]$ dataset. Results on a test beam with $r_{avg} = 0.5$

- $\Delta Q_{x,y} \propto (0.02 - 0.023)$

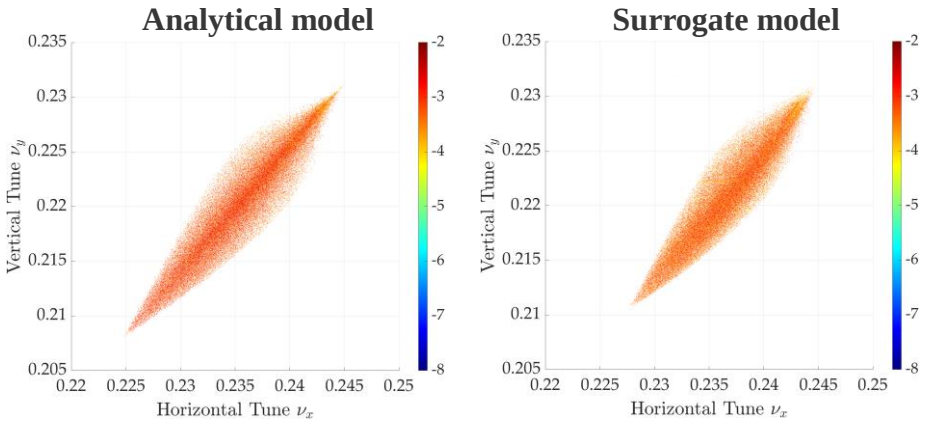


Fig.18 Tune diagram comparison.

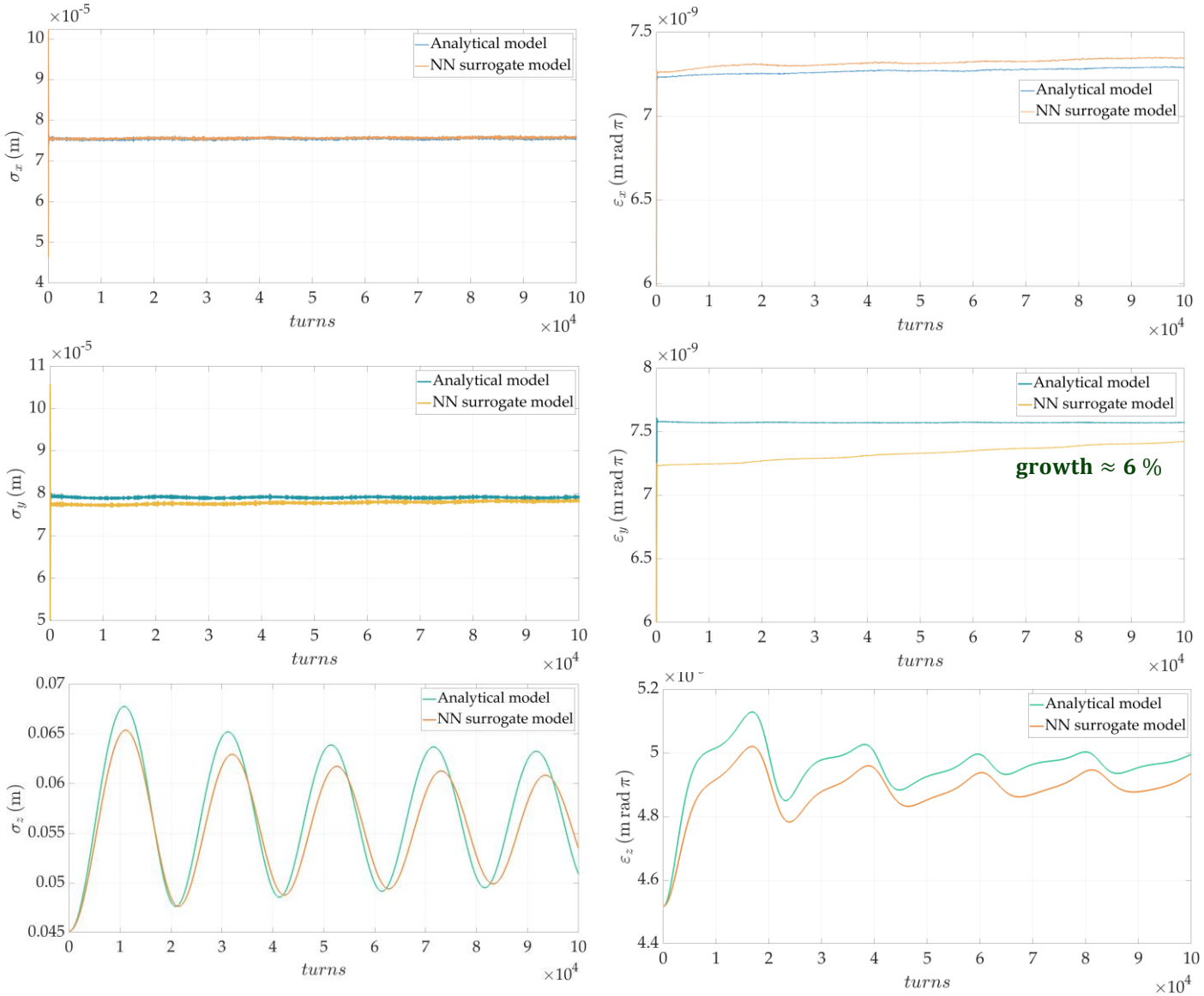


Fig.19 Envelope study, beam size and emittance evolution over 100,000 turns with 10x space charge force.

Conclusions

- A simple MLP symplectic neural network here presented can be used as a surrogate model.
- Future validation work:
  - Benchmark of the surrogate model vs. standard analytical methods for long term tracking ad multiple SC kicks.
  - The current network is effective for Gaussian beam distributions but lacks the resolution for arbitrary distributions and beam size. Ongoing work aims to resolve this, likely through a full 3D method.
- Long-term goals: this work can highlight the advantages of neural networks for long-term tracking calculations. The final aim is to generate a surrogate map that models space charge globally throughout the lattice, rather than just locally (similarly to the analytical models).



Thank you for your attention!





This material is based upon work supported by the U.S. Department of Energy, Office of Science, Office of Nuclear Physics and used resources of the Facility for Rare Isotope Beams (FRIB) Operations, which is a DOE Office of Science User Facility under Award Number DE-SC0023633.

References

[1] Bartosik, H., F. Asvesta, A. Huschauer, Y. Papaphilippou, and F. Schmidt. "Space charge induced losses in the CERN injector complex." Journal of Instrumentation 15, no. 07 (2020): P07021-P07021.

[2] Jeon, Dong-O., L. Groening, and G. Franchetti. "Fourth order resonance of a high intensity linear accelerator." Physical Review Special Topics—Accelerators and Beams 12, no. 5 (2009): 054204.

[3] Cousineau, S., S. Y. Lee, J. A. Holmes, V. Danilov, and A. Fedotov. "Space charge induced resonance excitation in high intensity rings." Physical Review Special Topics—Accelerators and Beams 6, no. 3 (2003): 034205.

[4] 3D gaussian distribution S. Kheifets notes

[5] Bassetti, M., and G. A. Erskine. n.d. *CLOSED EXPRESSION FOR THE ELECTRICAL FIELD OF A TWO-DIMENSIONAL GAUSSIAN CHARGE*.

[6] Qiang, Ji. 2025. “Two-and-a-Half Dimensional Symplectic Space-Charge Solver.” *Physical Review Accelerators and Beams* 28 (11): 114602. https://doi.org/10.1103/npx1-nclt.

[7] Meiss, James D. "Symplectic maps, variational principles, and transport." Reviews of Modern Physics 64, no. 3 (1992): 795.

[8] Svozil, Daniel, Vladimir Kvasnicka, and Jiri Pospichal. "Introduction to multi-layer feed-forward neural networks." Chemometrics and intelligent laboratory systems 39, no. 1 (1997): 43-62.

[9] https://github.com/ykkan/WSTrack.jl

[10] Jin, P., Zhang, Z., Zhu, A., Tang, Y., Karniadakis, G.E., 2020. SympNets: Intrinsic structure-preserving symplectic networks for identifying Hamiltonian systems.

[11] Li, Y., Xu, D., Hao, Y., 2025. Construction of approximate invariants for nonintegrable Hamiltonian systems. Phys. Rev. Accel. Beams 28, 074001.

[12] Karniadakis, George Em, Ioannis G. Kevrekidis, Lu Lu, Paris Perdikaris, Sifan Wang, and Liu Yang. "Physics-informed machine learning." Nature Reviews Physics 3, no. 6 (2021): 422-440.

[13] Zhang, Peixuan, and Zhiping Qiu. "Equation-driven generalized Hamiltonian neural networks with symplectic propagation for structural dynamics." Computational Mechanics (2026): 1-31.